RESPONSE ANALYSIS OF THE HIGASHI–KOBE BRIDGE AND SURROUNDING SOIL IN THE 1995 HYOGOKEN–NANBU EARTHQUAKE

TODOR GANEV[1], FUMIO YAMAZAKI[2]*, HIROSHI ISHIZAKI[3] AND MASAHIKO KITAZAWA[3]

[1]*Failure Analysis Associates, Inc., 149 Commonwealth Drive, Menlo Park, CA 94025, USA*
[2]*Institute of Industrial Science, The University of Tokyo, 7-22-1, Roppongi, Minato-ku, Tokyo 106, Japan*
[3]*Hanshin Expressway Public Corporation, 1-3-3 Higashi-Kawasaki-cho, Chuo-ku, Kobe 650, Japan*

SUMMARY

This paper presents results of observation and analysis of the response of one of the longest cable-stayed bridges in the world to the Hyogoken–Nanbu (Kobe) Earthquake of 17 January 1995. It is determined that interaction of the foundations of the bridge towers with the supporting soil plays a decisive role in the overall structural behaviour. The key factor governing the changes of the soil properties at this site is pore-water pressure buildup, which results in liquefaction of the saturated surface soil layers under large dynamic loads. Models of the soil and structure are created and initially validated by accurately simulating the system response to a small earthquake. Soil parameters reflecting the pore-water pressure buildup in the strong earthquake are determined by an advanced non-linear effective stress analysis, combining the Ramberg–Osgood model of stress–strain dependence with a pore pressure model based on shear work concept. They are utilized to investigate and simulate the interaction of the foundation and the supporting soil using the program SASSI with the flexible volume substructuring approach. The results show a good agreement with the observations and have useful implications to the scientific and engineering practice. © 1998 John Wiley & Sons, Ltd.

KEY WORDS: dynamic soil–structure interaction; Hyogoken–Nanbu Earthquake; cable-stayed bridge; pore-water pressure buildup; liquefaction analysis

INTRODUCTION

The Higashi–Kobe Bridge in Kobe City, Japan, is one of the longest cable-stayed bridges in the world. It is a part of one of the most important transportation arteries in Japan—The Osaka Bay Route, which is an 80 km expressway stretching from the western end of Kobe to the southern end of Osaka (Figure 1). The Higashi–Kobe Bridge spans the Higashi–Kobe Channel connecting two reclaimed land areas: Uozaki-hamamachi on the west and Fukae-hamamachi on the east (Figure 1). The Higashi–Kobe Channel is 500 m wide and has a 455 m seaway where large ferries frequently pass and maneuver to dock at the nearby Ohgi Ferry Terminal.

At 5:46 a.m. on 17 January 1995, Kobe was struck by the most devastating earthquake[1] to strike Japan since the Great Kanto Earthquake of 1923. Its epicentre was located at $34° 36''$N and $135° 00''$E. The JMA magnitude of the earthquake was 7·2, its surface wave magnitude M_S was 7·2 and the moment magnitude M_W was 6·9. The focal depth was 14 km. This paper presents results of observation and analysis of the behaviour of the Higashi–Kobe Bridge during the Hyogoken–Nanbu (Kobe) Earthquake.

As will be shown in the following discussion, a simulation of the bridge response needs to take into account the soil–structure interaction. Engineering experience has shown that in addition to the well-developed

---

* Correspondence to: Fumio Yamazaki, Institute of Industrial Science, The University of Tokyo 7-22-1, Roppongi, Minato-ku, Tokyo 106, Japan. E-mail: yamazaki@iis.u-tokyo.ac.jp
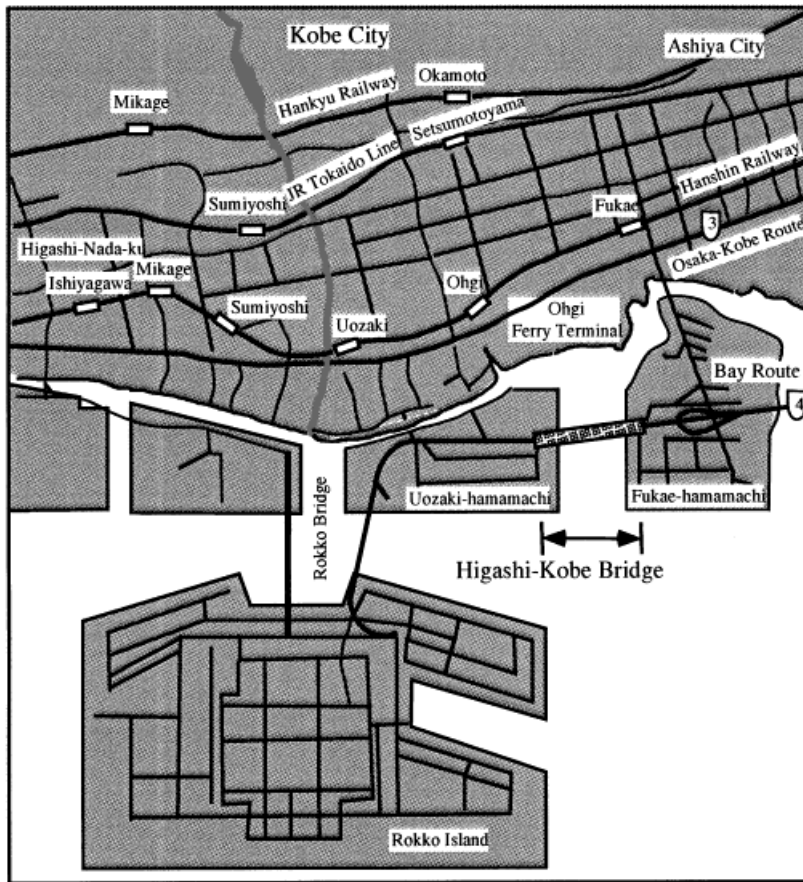
Figure 1. Location of the Higashi–Kobe Cable-Stayed Bridge

theoretical basis of soil–structure interaction, it is necessary to validate the approaches in comparison with observed data and correct the numerical models to consider discontinuities and non-linearities. One of the most important practical issues associated with interaction analysis is the degradation of the supporting soil due to large dynamic excitations. In general, three factors[2] are considered most influential to the soil stiffness degradation: non-linear stress–strain dependence of the soil material, separation of soil from the structure and pore-water pressure buildup. The relative importance of each of these factors varies with each analysed case and usually determines the methodology of analysis.

The present authors have already published results of case studies in which the most influential factor has been the separation of soil from the structure,[3] and in which the decisive role has been played by soil nonlinearity.[4] Of particular interest in the present case is that the key factor to soil-stiffness degradation is the pore-water pressure buildup. Publicized data of actual soil and structural response including this complicated phenomenon are not widely available.

The pronounced non-linear effects accompanying pore-water pressure buildup and liquefaction are time-dependent. Non-linear dynamic solutions in the time domain only for soil or for structural response are readily available and their practical application is feasible. However, when the interaction of soil and structure is addressed, it is also important to consider the frequency dependence of the soil parameters. For this reason, and to decrease the computational effort and data storage requirements, most of the commercially available programs such as SASSI[5] operate in the frequency domain with time-independent parameters. In

this way, it appears that the most practical way to analyse soil–structure interaction would be to determine equivalent time-independent parameters on the basis of a more rigorous solution and input them into a typical interaction analysis program. Obviously, separate sets of equivalent parameters are necessary to capture the system behaviour in the small and large strain ranges. This approach was adopted in the present study.

CHARACTERISTICS OF THE HIGASHI–KOBE BRIDGE

The Higashi–Kobe Bridge has been designed[6] by the Hanshin Expressway Corporation. The consultant services of Sogo Engineering Inc., Osaka, have been subcontracted to perform seismic analysis. Figure 2 presents a scheme of the eastern-half of the bridge, which has three spans and a total length of 885 m. The centre span measures 485 m and the side spans are 200 m each. The bridge piers at the east side are named P24, P25 and P26. Accelerometers are placed on three location on the tower at P24. They are designated by T1, T2 and T3 in Figure 2. The soil response during earthquakes is recorded by accelerometers buried in the ground at depths 34 (G1 in Figure 2) and 1·5 m (G2 in Figure 2) at a 50 m distance from the foundation at P24. An accelerometer is also installed at the bottom of the caisson (K1 in Figure 2).

The specifications of the bridge and its components are summarized in Table I. The steel deck is an orthotropic slab structure with deck plates of thickness 12 mm, reinforced with longitudinal ribs at 70 cm intervals and transverse ribs at 3 m intervals. Its cross-section is shown in Figure 3.

An outstanding feature of the Higashi–Kobe Bridge is that the main girder can move longitudinally on all supports with the corresponding displacements restricted mainly by the cables. This provides an unusually long predominant period of sway mode oscillation—approximately 4·4 s. The largest values of design
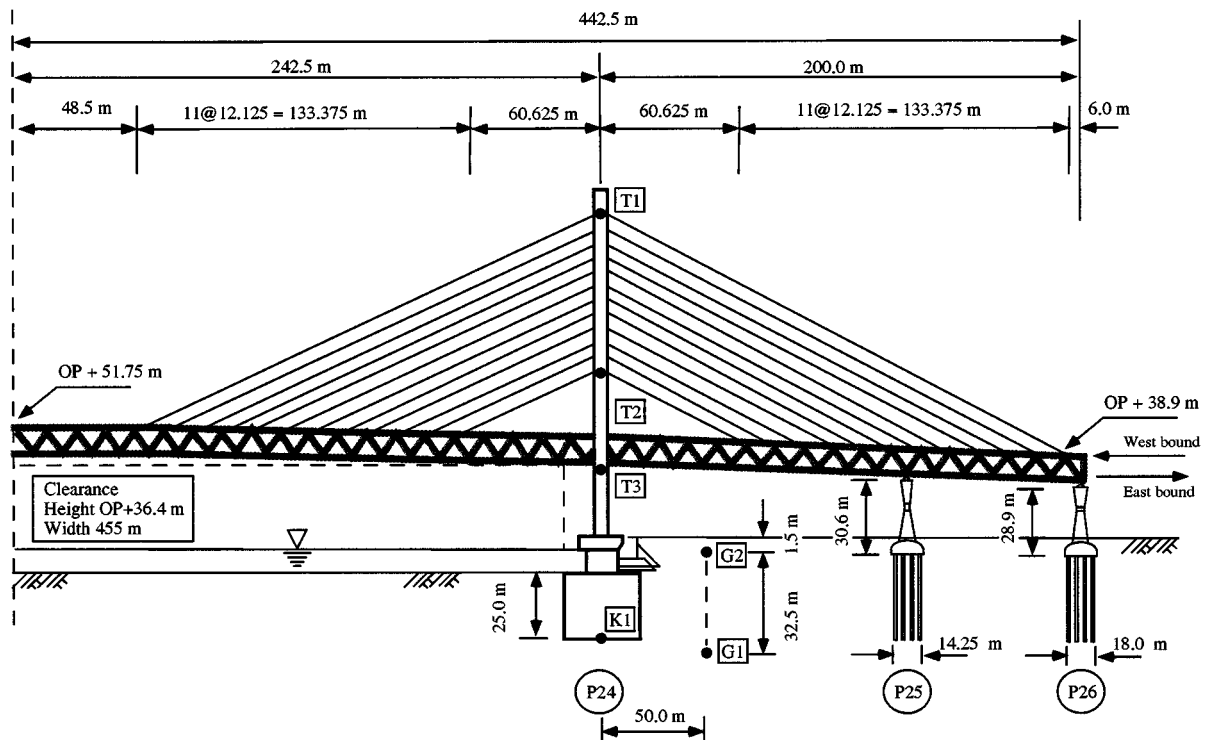

Figure 2. Scheme of the bridge and locations of the seismometers

Table I. Specifications of the Higashi–Kobe Bridge

| Type	Three-span continuous steel cable-stayed bridge		
Road category	Group 2, Class 1 (Japan Road Association Specifications[7])		
Design velocity	80 km/h		
Roadway	2 decks × 3 lanes		
Length	200 + 485 + 200 = 885 m		
Width	13·5 m × 2 decks		
Tower	H-shaped tower (146·5 m)		
Main girder	Warren truss (height 9 m)		
Cables	Harp pattern multi cable (12 cables in a plane)		
Substructure	Caisson foundation (for towers)		
	Pile foundation (for piers)		
Weight of the superstructure	Main girder	141 000 kN	
	Towers	79 000 kN	
	Cables	13 000 kN	Total: 274 000 kN
	Piers	17 000 kN	
	Others	24 000 kN	
Specifications of the caissons	Weight of the steel shells	9500 × 2 = 19 000 kN	
	Volume of the concrete	15 300 × 2 = 30 600 m^3	
	Weight of the reinforcing bars	13 000 × 2 = 26 000 kN	
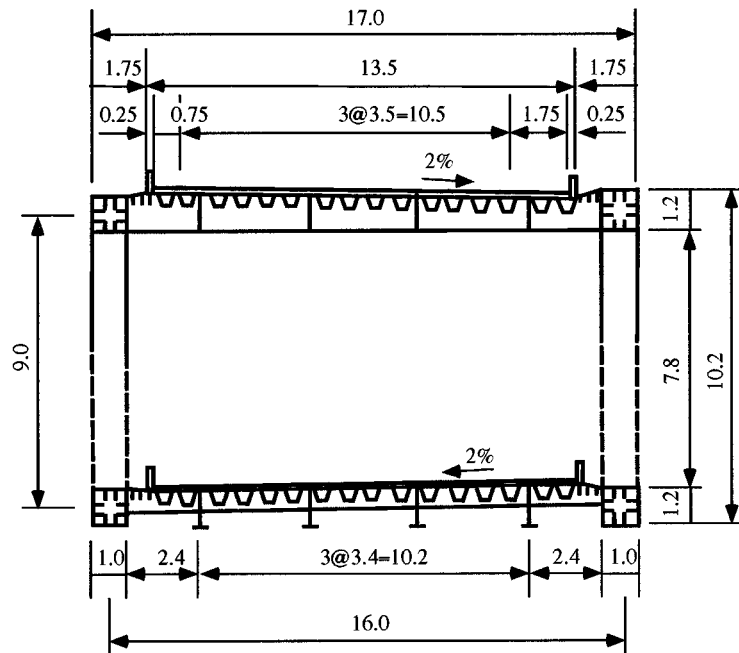
Figure 3. Cross-section of the main girder (dimensions in m)

earthquake response spectra, prescribed by the standard code or formulated specifically for other large bridges in Japan, fall typically in the range 0·2–2·5 s.[7] Consequently, placing the natural period of the Higashi–Kobe Bridge outside this range contributes to seismic safety and enables economical and elegant design of the bridge towers. Wind shoes installed on the towers and the piers are designed in such a way that
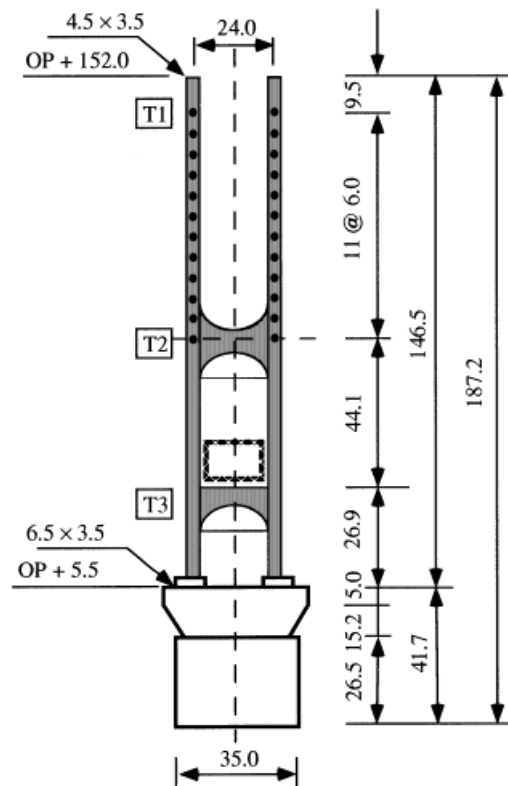
Figure 4. Scheme of the tower at P24 (dimensions in m)

the longitudinal motion of the main girder is not inhibited by the friction between the shoe components when the bridge is subjected to diagonal forces. Eye-bar pendulum supports are used for the side span piers to reduce the centre span deflection by live loads.

The number of cables (96 in total) is sufficiently large to result in low tension in each of them, and this allows the use of small cable anchors, which are encased in the truss chord members. Each cable consists of 241–301 wires of diameter 7 mm. They are clad in polyethylene tubes for protection from corrosion. Since wind- and rain-induced vibration have been reported on other bridges with polyethylene-covered cables, an unique measure has been taken to alleviate this problem for the Higashi–Kobe Bridge. After numerous experiments in wind tunnels it has been established that attaching protuberances parallel to the cable axis would control the vibrations by directing the rain drops in rivulets down the cable cover.

The bridge towers are H-shaped and have heights of 146·5 m. The cross-section of each tower column measures $3·5 \times 6·5$ m at the base and $3·5 \times 4·5$ m at the top. The horizontal distance between the two columns is 24 m. A scheme of the tower at bridge pier P24 is presented in Figure 4. The columns are constructed using hollow steel elements with rectangular cross-section, which are joined by welding. High-strength bolt joints are used at five locations per column to correct uneven shrinkage due to welding.

The tower foundations are pneumatic caissons of size 35 (W) $\times$ 32 (L) $\times$ 26·5 (H) m. A vertical and two horizontal cross-sections of the foundation at P24 are shown in Figure 5. The inside of each caisson is divided into 6 rows of 6 cells with partition walls. The foundations have been constructed by the floating caisson method. The steel shells of the caisson have been connected with the reinforcing bars and used as molds for the concrete foundation. The secondary piers at the side spans are founded on piles.
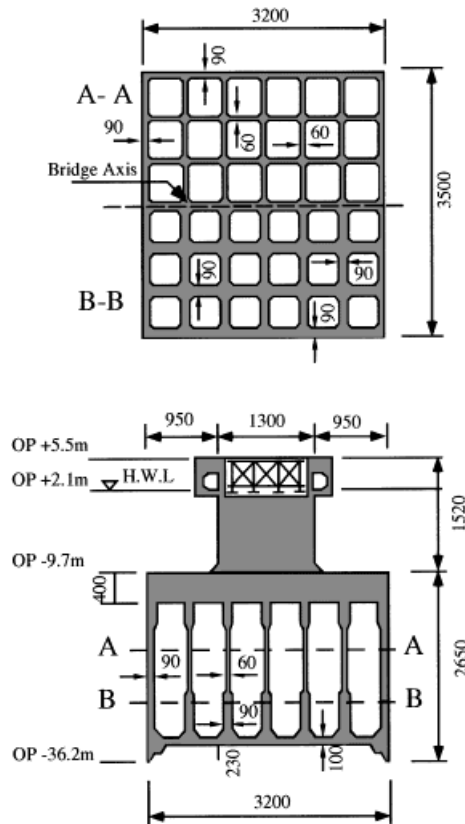
Figure 5. Horizontal and vertical cross-sections of the foundation at P24 (dimensions in cm)

Numerous tests have been performed by the Hanshin Expressway Corporation to evaluate the properties of the soil around the foundations. Figure 6 shows a model of the soil profile at P24, which reflects the results of the comprehensive geotechnical investigations. The soil structure is very complicated and consists of interlacing layers of gravel, sand and clay with substantially varying characteristics.

OBSERVED RESPONSE OF THE BRIDGE AND THE SURROUNDING SOIL

The 1995 Hyogoken–Nanbu earthquake

Figure 7 presents time histories of acceleration response of the Higashi–Kobe Bridge and the surrounding soil during the 1995 Hyogoken–Nanbu (Kobe) Earthquake. The records at the top (T1, cf. Figure 2) are overcalled, and are not shown in the figure. The transverse component at point T2 is also slightly overcalled. The maximum accelerations, velocities and displacements at each observation point are presented in Table II. As can be seen from the time history of the downhole accelerometer G2 (GL-34·0 m, cf. Figure 2), the near-fault ground motions include large pulses with long period, which are potentially damaging to multistorey buildings and bridges. Despite this harsh test, the Higashi–Kobe Bridge performed outstandingly during the Kobe Earthquake. The only sustained damage was to a wind shoe at one of the secondary piers on the west side in Uozaki-hamamachi.

The time history of acceleration at the main girder level (T3, Figure 7(c)) shows multiple pulses followed by decaying vibrations towards the coda of the record. If a cable has been relaxed in a certain moment and its

Ordinate from OP (m)	Soil Type	Layer thickness (m)	SPT N value	Unit weight γ (kN/m³)	Poisson ratio ν	Cohesion c (kN/m²)	Internal friction angle ϕ (degrees)	Shear modulus G (kN/m²)	Shear wave velocity (m/s)	Grain size $D50$ (mm)	Fine contents (%)
5.31 / -1.69	①	7.00	10	18.0	0.48	0.0	36.0	47020	160.0	2.20	9.0
-1.69 / -8.29	①	6.60	15	18.0	0.44	0.0	36.0	154470	290.0	2.20	9.0
-8.29 / -18.49	①	10.20	20	19.0	0.49	0.0	32.0	154470	290.0	2.70	5.0
-18.49 / -21.64	①	3.15	17	19.5	0.48	0.0	31.0	198530	320.0	1.50	10.0
-21.64 / -25.34	③	3.70	43	19.5	0.47	0.0	41.0	272400	370.0	2.50	12.0
-25.34 / -29.09	②	3.75	29	19.5	0.49	23.2	3.0	114610	240.0	0.03	80.0
-29.09 / -31.64	③	2.55	50	19.5	0.48	0.0	42.0	230020	340.0	2.10	13.0
-31.64 / -33.74	②	2.10	18	19.5	0.49	14.4	3.0	87750	210.0	0.10	57.0
-33.74 / -37.39	③	3.65	50	19.5	0.49	5.0	40.0	334480	410.0	0.79	12.0

Soil types : ① Alluvial sands ; ② Diluvial clay ; ③ Diluvial sand

Figure 6. Soil model at P24

tensile resistance has been engaged in the next moment, the sudden restriction on the motion of the main girder will load the structure with an impulse. The occasional pounding with the adjacent part of the highway should be expected to cause a similar effect.

Comparing the time histories recorded by the downhole soil accelerometer G1 (GL-34·0 m) and the surface accelerometer G2 (GL-1·5 m, cf. Figure 2), it can be seen that the acceleration at the surface is smaller than the one at 34 m depth and exhibits longer period motion. These observations suggest that the surface soil layers, which consist of loose saturated sands, have been liquefied during the earthquake. This hypothesis is confirmed numerically in the following discussion. Evidently, within the duration of the event, the soil
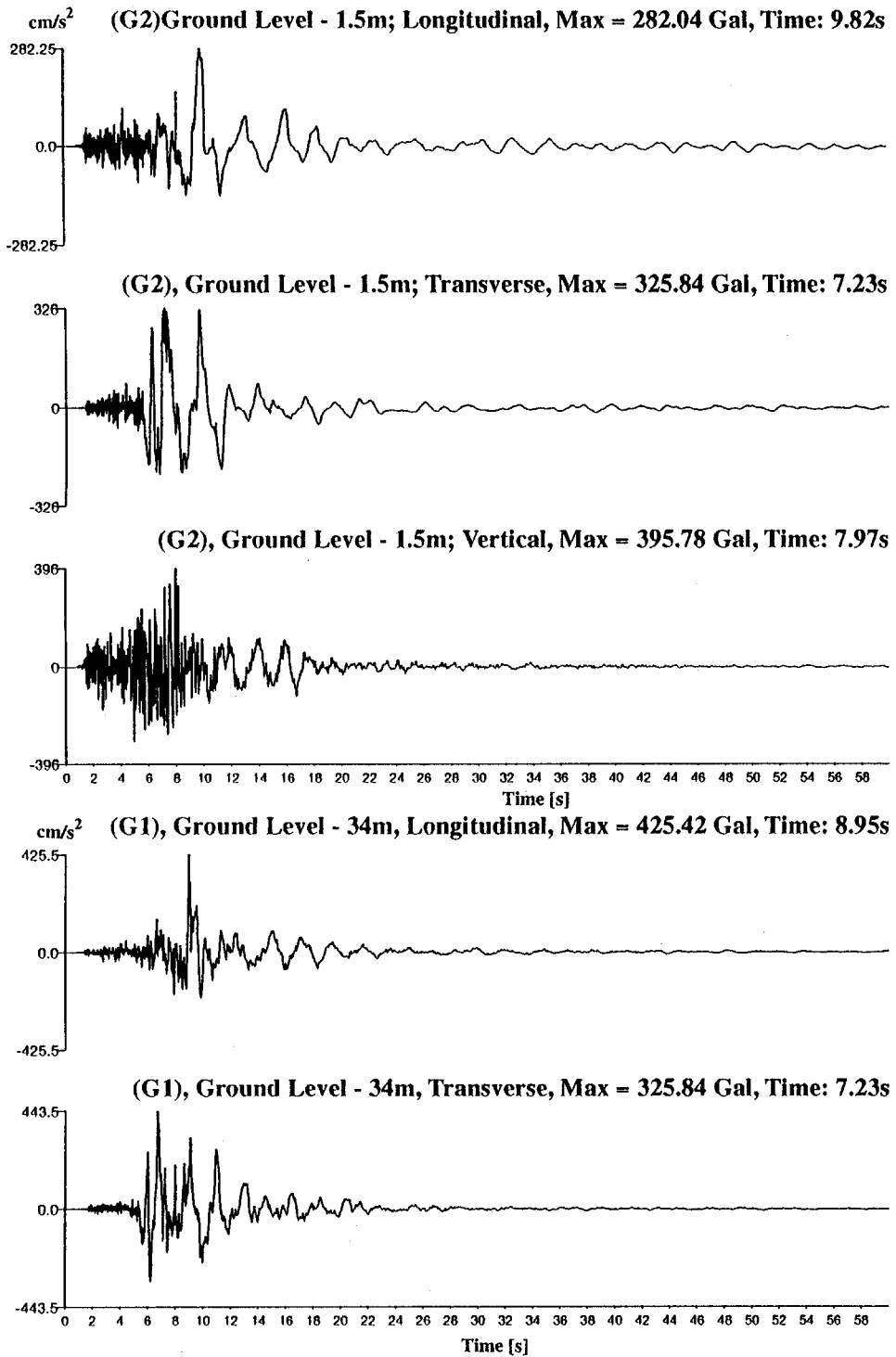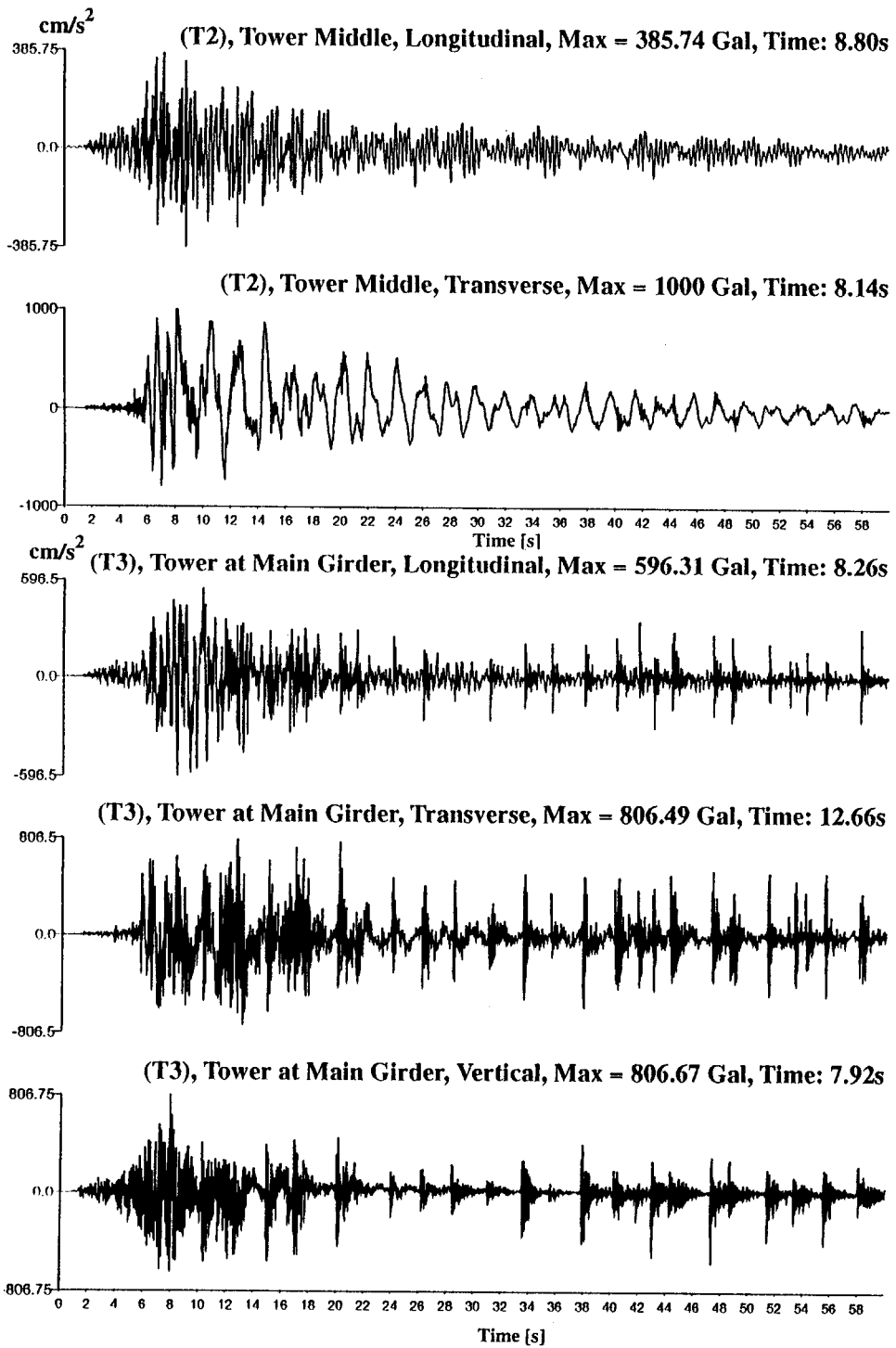
a) Downhole and surface soil

Figure 7. Time histories of acceleration of the Hyogoken–Nanbu Earthquake: (a) downhole and surface soil; (b) bottom of caisson foundation at P25; (c) Tower response at middle and main girder levels
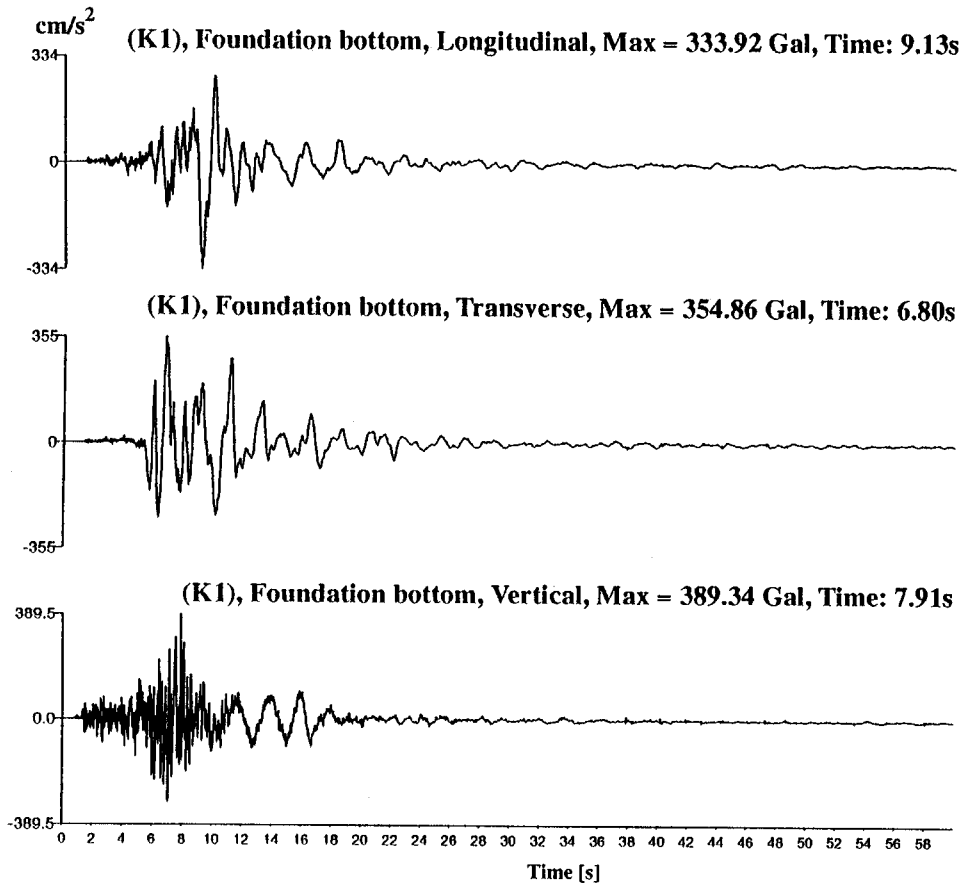
b) Bottom of caisson foundation at P25

Figure 7. *Contd.*

c) Tower response at middle and main girder levels

Figure 7. *Contd.*

Table II. Maximum recorded response to the 1995 Hyogoken–Nanbu Earthquake

Name and position	Orientation	Acceleration (cm/s^2)	Velocity (cm/s)	Displacement (cm)
G1 (GL − 34 m)	Longitudinal	425·4	71·2	27·8
	Transverse	443·4	76·0	34·3
G2 (GL − 1·5 m)	Longitudinal	282·0	84·5	51·2
	Transverse	325·8	90·7	49·5
	Vertical	395·8	35·0	14·9
K1 (Bottom of foundation at P24)	Longitudinal	333·9	77·5	34·0
	Transverse	354·9	79·1	39·4
	Vertical	389·3	34·1	12·6
T2 (Middle of tower at P24)	Longitudinal	385·7	29·1	18·7
	Transverse	1000*	225·1[†]	117·6[†]
T3 (Tower at P24, level of main girder)	Longitudinal	596·3	90·7	33·9
	Transverse	806·5	105·7	51·3
	Vertical	806·7	71·1	37·8

* Overscaled gauge

[†] The value is calculated from an overscaled record

a) Ground level -1.5 m, longitudinal component

b) Ground level -34.0 m, longitudinal component
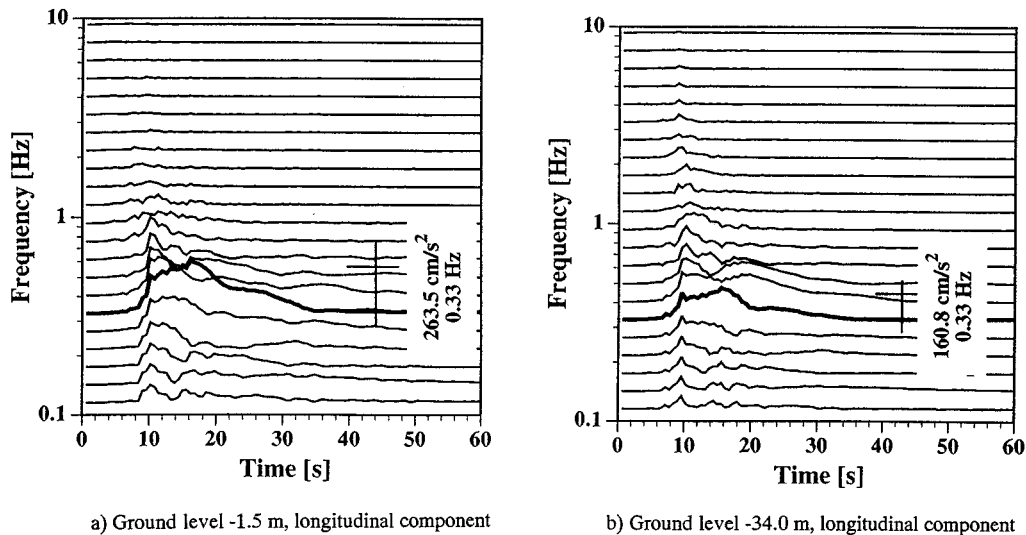
Figure 8. Evolutionary response spectra of ground motion: (a) Ground level − 1.5 m, longitudinal component; (b) Ground level − 34.0 m, longitudinal component

properties underwent significant changes. Non-stationary response analysis was performed to investigate the effects of these changes for the purposes of numerical simulation of the soil–structure system behaviour. Figure 8 presents evolutionary response spectra of the longitudinal motion at depth 34 m and at the ground surface. It can be seen that the peak values diminish at frequencies above 5 Hz and outside of the time interval 10–20 s.

Figure 9 offers results of stationary analysis of the same records. It compares Fourier spectrum ratios between the downhole and the surface acceleration for three time intervals. In the initial 5 s, amplification is
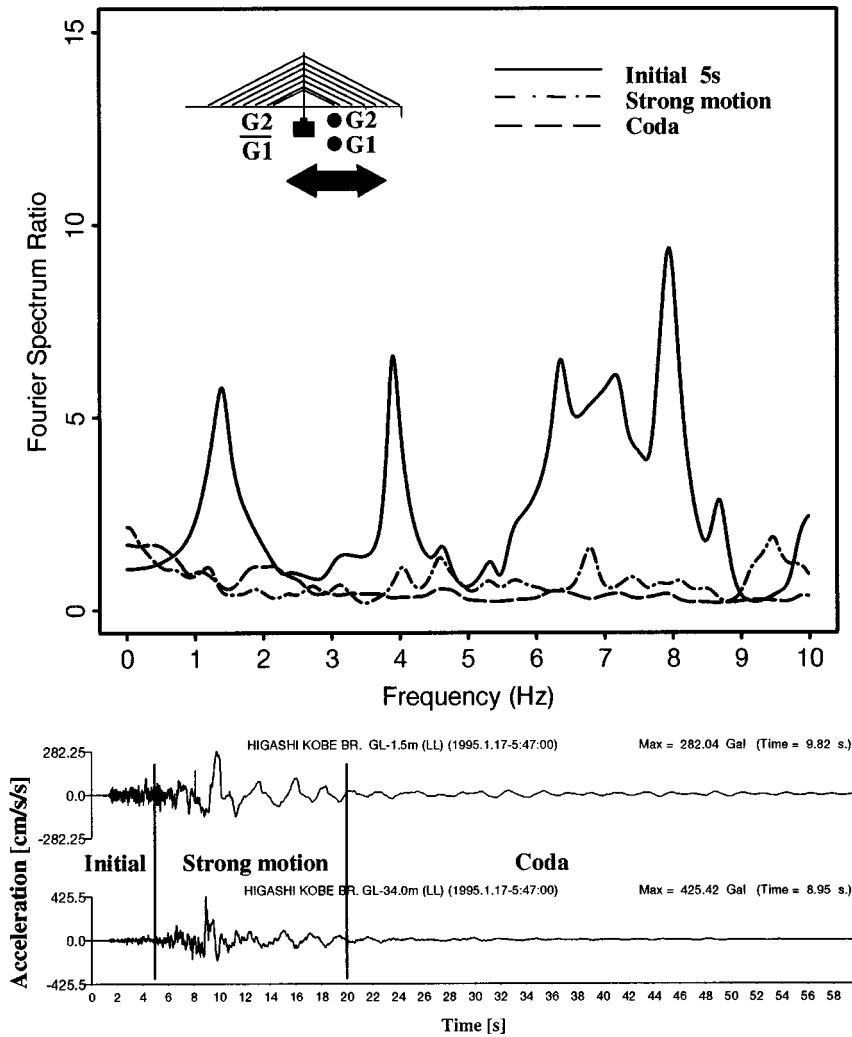
Figure 9. Fourier spectrum ratios between surface and downhole ground acceleration records (longitudinal direction)

observed. During the strong motion, the amplitude ratios are much lower, which can be explained with the occurrence of liquefaction. At the coda of the record, it is hypothesized that complete liquefaction of the surface layers greatly suppresses the energy transfer. Similar results are obtained by analysis in the transverse direction.

Comparison with a small earthquake

To assess the effect of the soil–structure interaction effects in a large earthquake a comparison was made with the behaviour of the system in a small event, which occurred on 25 January 1996 and had a peak ground acceleration of 42·5 cm/s². Its characteristics are summarized in Table III. Figure 10 presents Fourier spectrum ratios between the free field at depth 34 m and the mid-height of the bridge tower, evaluated from the records of the Hyogoken–Nanbu Earthquake and from the small event. Since the tower is tall, slender and flexible, its elastic response dominates the total response and sway and rocking modes of motion have a secondary influence. In this way, the soil stiffness degradation does not lead to substantial shift of the

Table III. Maximum recorded response to a small earthquake of January 1996

| Name and position	Orientation	Acceleration (cm/s^2)	Velocity (cm/s)	Displacement (cm)
G1 (GL − 34 m)	Longitudinal	25·0	1·5	0·13
	Transverse	23·0	1·5	0·07
G2 (GL − 1·5 m)	Longitudinal	42·0	2·6	0·26
	Transverse	31·0	1·6	0·13
	Vertical	24·0	1·0	0·07
K1 (Bottom of foundation at P24)	Longitudinal	15·0	1·5	0·15
	Transverse	13·0	1·0	0·08
	Vertical	13·0	0·9	0·04
T2 (Middle of tower at P24)	Longitudinal	31·0	1·5	0·09
	Transverse	11·0	1·6	0·14
T3 (Tower at P24, level of main girder)	Longitudinal	66·0	3·8	0·32
	Transverse	65·0	1·9	0·13
	Vertical	19·0	0·9	0·05
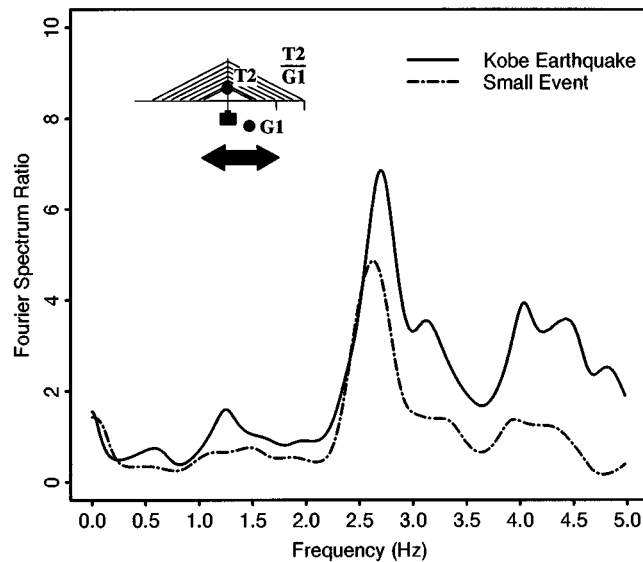
Figure 10. Comparison of Fourier spectrum ratios evaluated from large and small earthquakes (longitudinal direction)

predominant frequency of the system, as is often observed for shorter, squatter and rigid structures.[3,4,8] The alteration of the soil behaviour affects mainly the amplitude of the response.

NUMERICAL SIMULATION OF DYNAMIC RESPONSE

Modelling considerations

Considering the necessity to take into account soil–structure interaction, analysis was performed with the program SASSI employing the flexible volume substructuring approach.[5] Taking advantage of the symmetry, a quarter model of the bridge was used. Based on the observations in the previous section, it was
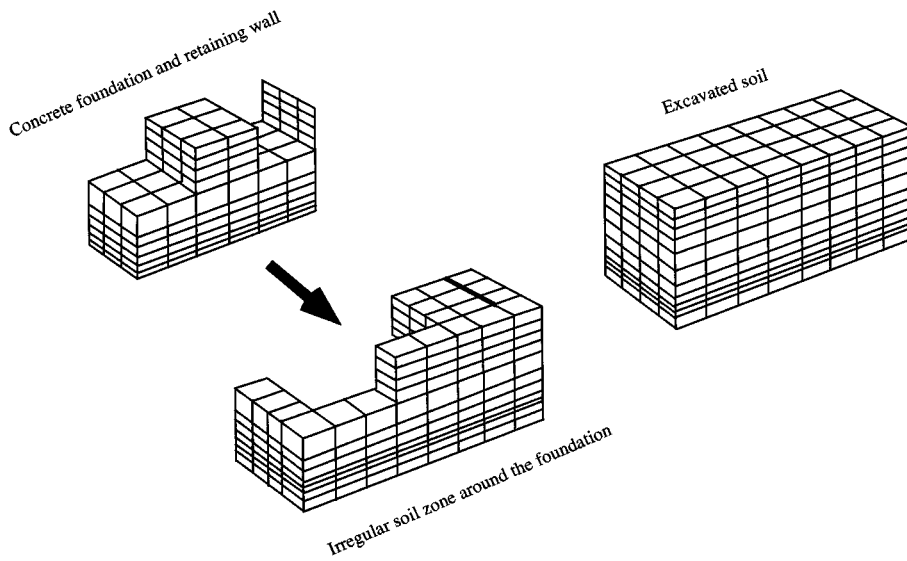
Figure 11. Discretization of the foundation and near-field soil at P24 by the flexible volume substructuring approach
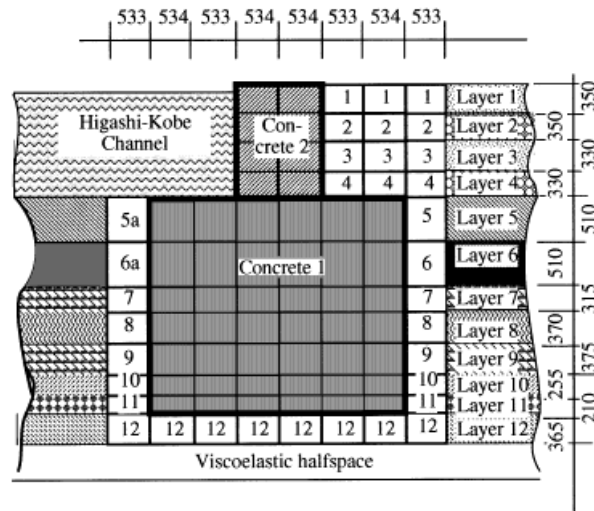

Figure 12. Vertical cross-section of the soil and foundation model

determined that an adequate frequency range for analysis would be up to 5 Hz. As the maximum frequency of analysis also determines the maximum size of the finite elements, this choice also led to a reasonably efficient model. A conceptual scheme of the discretization of the foundation and the near-field soil with solid prismatic elements is shown in Figure 11. Figure 12 shows a cross-section of the same region and indicates the soil types. The characteristics of each soil type can be found in Table IV for different analysis stages. Determination of parameters for the Hyogoken–Nanbu Earthquake is discussed in the following sections.

The superstructure was modelled with beam elements with the mass concentrated in their nodes to avoid lengthy calculations and large memory and storage requirements, which would be imposed by discretizing

a) Main girder, cables and supports
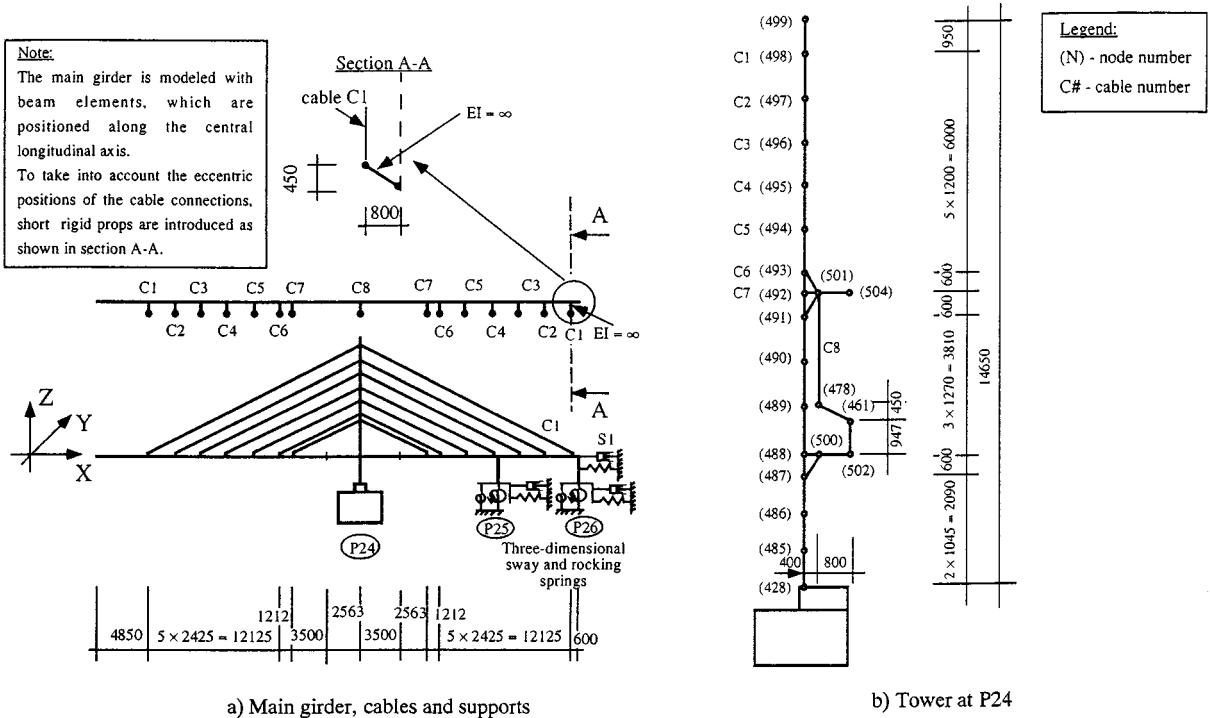
b) Tower at P24

Figure 13. Finite element discretization of the superstructure: (a) Main girder, cables and supports; (b) Tower at P24

the truss according to its members (Figure 13). The fact that the cables are attached to both sides of the main girder, at a distance of 8 m away from the longitudinal axis, was considered by attaching a lateral beam support with infinite rigidity for each cable. They are shown in the enlarged section in Figure 13(a). The current version of SASSI does not include finite elements for piles in its library, although such are planned in the further development of the program. For this reason, the pile foundations were represented by equivalent three-dimensional generalized sway and rocking springs, as shown in Figure 13(a). The spring S1 is added to consider, in an approximate manner, the pounding of the structure with the adjacent part of the highway.

An additional modelling consideration was the cable action, since the only appropriate elements in the SASSI library are of beam type and have compression stiffness. The effect of the error of using beam elements for modelling of the cables was investigated with the program MSC/NASTRAN,[9] using as dynamic excitation for the small earthquake of January 1996 (Table III). The cables were modelled once with a combination of gap and spring elements and non-linear dynamic analysis was performed, considering the initial tensile stress in the elements due to gravity. The solution was compared to a linear solution with beam elements. It was found that with the given geometrical disposition of the cables, the tension forces in them from gravity are large enough to create effective compression resistance almost equal to their tensile stiffness. In this way it was judged that linear analysis with beam elements would be a reasonable approximation and it is justifiable to use SASSI. Obviously, the error would depend on the magnitude of the displacements and would be larger for a stronger earthquake. For the MSC/NASTRAN analysis only, the soil support at the P24 foundation was modelled with equivalent three-dimensional generalized springs, evaluated on the basis of the Continuum Formulation Method.[3,4,10] As the main purpose of these calculations was to validate the superstructure model, the soil spring action is not discussed here.
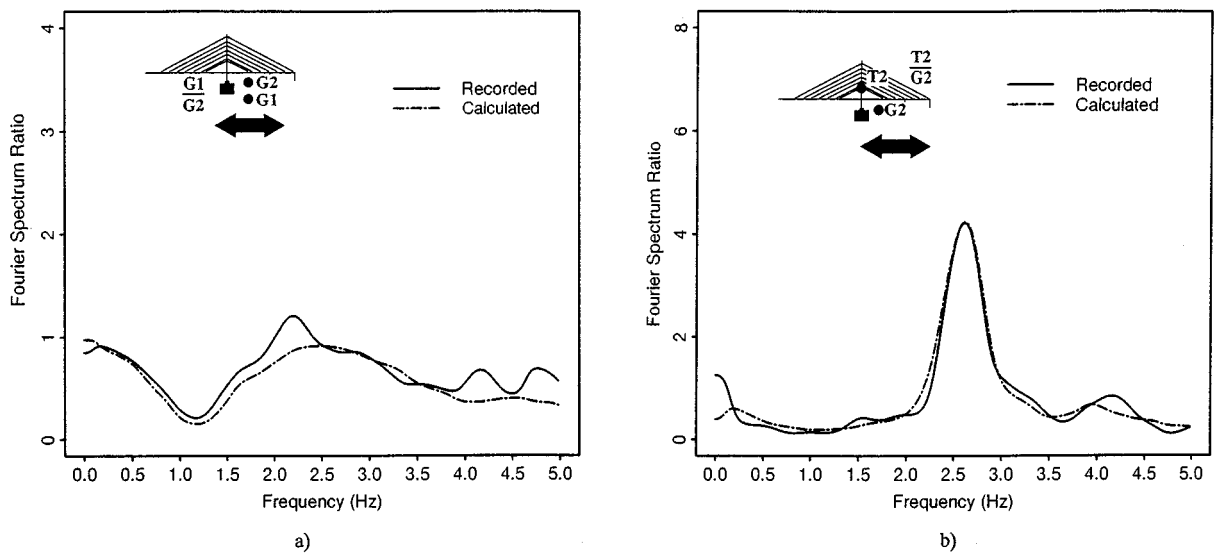
Figure 14. Simulated and recorded Fourier spectrum ratios for a small earthquake

Small-strain linear dynamic response

At the initial stage of the analysis, the behaviour of the soil–structure system in the small-strain linear range was examined by simulating its response to the small earthquake described by Table III. Equivalent stiffness and damping characteristics of the soil were determined using the program SHAKE on the basis of the one-dimensional wave propagation theory. The results of this analysis validated the use of initial soil properties as well as the model of the superstructure. In conjunction with non-linear dynamic analysis performed with MSC/NASTRAN, it helped determine the modelling of the cable action as discussed in the previous section. Figure 14(a) compares the Fourier spectrum ratio of the recorded surface and downhole soil records with those calculated by SASSI. The good agreement signifies that the soil model is adequate. Figure 14(b) shows the recorded and calculated Fourier spectrum ratios between the free field surface and the mid-height of the tower. The excellent correlation validates the superstructure model.

Dynamic response in the large-strain range

Analysis of the soil response in the main shock of the Hyogoken–Nanbu Earthquake with SHAKE produced inadequate results and an alternative method of determination of equivalent soil properties was necessary. The non-linear behaviour of the soil was investigated with a one-dimensional effective stress analysis program.[11] In this simulation, the Ramberg–Osgood model[12] of stress–strain soil dependence is combined with a pore pressure buildup model based on shear work concept[13,14] to iteratively obtain soil characteristics and response in the time domain.

The input motion was specified by the acceleration record at depth 34 m. Figure 15 shows a very good agreement between recorded and simulated soil response at the ground surface. The occurrence of liquefaction has been captured adequately by the model. Figure 16 shows a comparison between the maximum values of the excess pore-water pressure and initial effective stress. It is evident that the soil was completely liquefied down to a depth of approximately 6 m, which confirms the hypothesis formulated in the previous section. To a depth of 10 m the ratio of excess pore-water pressure to initial effective vertical stress is about 86 per cent, indicating that the soil in that region came to a state close to liquefaction. The time history of the ratio of the excess pore water pressure to the initial effective stress in the surface layer is plotted in Figure 17.
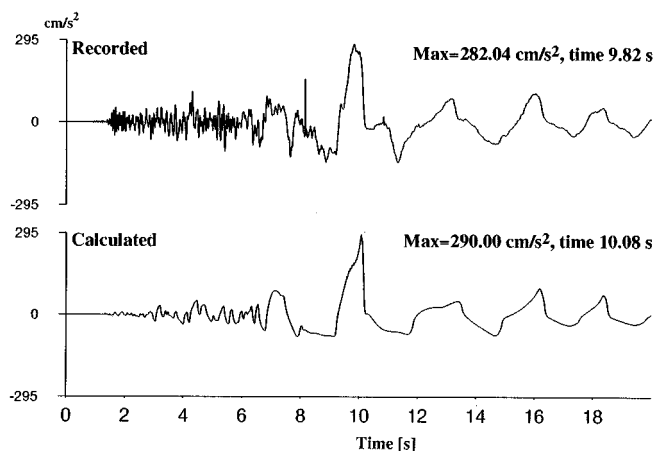
Figure 15. Time history of recorded and simulated acceleration response at the ground surface (longitudinal component)
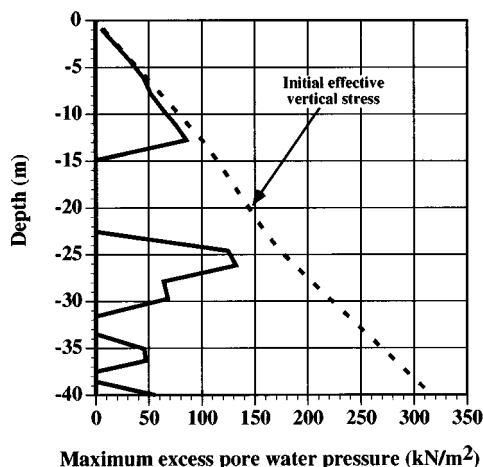

Figure 16. Distribution of maximum excess pore water pressure with depth by the effective stress response analysis

The results of the non-linear soil response analysis were utilized in determining the soil properties used in the soil–structure interaction analysis. It should be pointed out that for the period of the strong earthquake motion the soil stiffness cyclically goes through stages of severe degradation, followed by stages of temporary recovery. On the other hand, the program SASSI requires linear parameters for input. For this reason, equivalent linear properties of the soil layers were determined based on the time-dependent values obtained by the soil response analysis. The stiffness parameters were calculated by averaging the time-varying stiffness in the period 8–10 s (cf. Figure 7). The damping ratios, which are also strain-dependent, were averaged for the same time window. As the primary objective is to simulate the system response to the strong-motion part of the earthquake, this approximation was found appropriate. Note that non-linear soil–structure interaction analysis would be too difficult for the present analysis in many aspects. The equivalent soil parameters are listed in Table IV. The time history of deep ground acceleration was used for seismic input as deconvolution of the surface record would be inaccurate under the conditions of liquefaction.

Figure 18 compares the recorded and calculated Fourier spectrum ratios between the deep ground motion and the response of the bridge tower at P24 at mid-height. The agreement is reasonably good, albeit worse
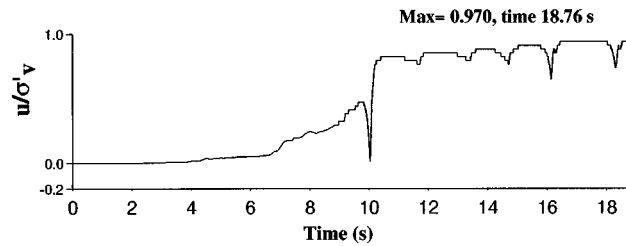
Figure 17. Time history of the ratio of the excess pore-water pressure to the initial effective stress by the effective stress analysis

Table IV. Soil properties used for dynamic analysis in longitudinal direction

Soil type	Small earthquake				The Hyogoken–Nanbu Earthquake			
	Shear wave velocity V_S (m/s)	Poisson ratio v	Unit weight γ (kN/m³)	Damping ratio D (%)	Shear wave velocity V_S (m/s)	Poisson ratio v	Unit weight γ (kN/m³)	Damping ratio D (%)
1	151	0·48	18·0	3·3	20	0·48	18·0	12·0
2	144	0·48	18·0	5·6	30	0·48	18·0	12·0
3	271	0·44	18·0	3·6	40	0·44	18·0	12·0
4	269	0·44	18·0	4·0	40	0·44	18·0	12·0
5	107	0·49	16·0	5·3	70	0·49	16·0	10·0
5a	107	0·49	15·0	5·3	70	0·49	15·0	8·0
6	116	0·49	16·0	3·8	50	0·49	16·0	10·0
6a	116	0·49	15·0	3·8	50	0·49	15·0	10·0
7	302	0·48	19·0	3·2	234	0·48	19·0	5·0
8	363	0·47	19·5	2·8	297	0·47	19·5	3·3
9	238	0·49	19·5	0·4	196	0·49	19·5	3·0
10	331	0·48	19·5	3·0	317	0·48	19·5	7·1
11	207	0·49	19·5	0·7	198	0·49	19·5	7·1
12	410	0·49	19·5	0·2	380	0·49	19·5	7·1

than in the case of the small-strain response. It is evident that the equivalent linear soil parameters are not capable of producing a perfect simulation of the complicated non-linear behaviour, but offer a reasonable accuracy for practical purposes. The difference between recorded and calculated response in the range 4–5 Hz can be explained with the fact that the equivalent averaged soil properties cannot take into consideration the temporary recovery of soil stiffness during dynamic loading cycles and thus some of the higher-frequency contents cannot be simulated adequately.

CONCLUSIONS

The response of the Higashi–Kobe Bridge during the Hyogoken–Nanbu (Kobe) Earthquake of 17 January 1995 was analysed with a finite element model employing flexible volume substructuring approach. Equivalent linear parameters for soil–structure interaction analysis with the program SASSI were determined by a non-linear dynamic effective stress analysis for layered ground. The applied methodology aimed to simulate the complicated non-linear soil and structural behaviour separately and rigorously.

Both non-stationary and stationary analysis of the observed accelerograms were applied to identify the key phenomena affecting the performance of the bridge and the surrounding soil.
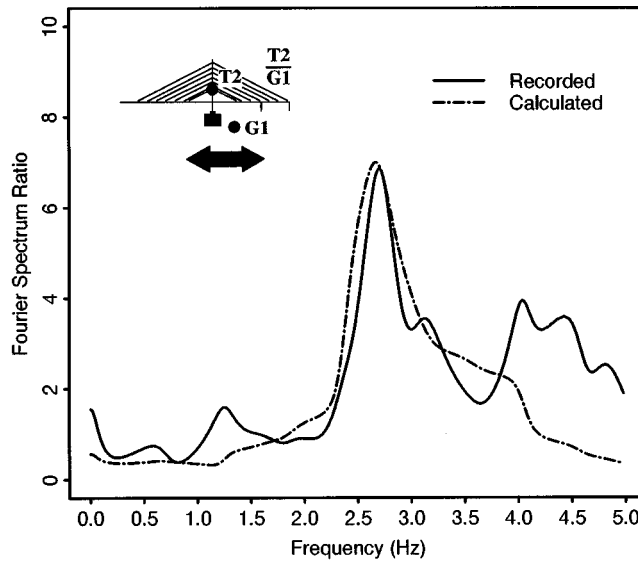
Figure 18. Simulation of the response to the 1995 Hyogoken–Nanbu Earthquake

Soil and superstructure models were created and initially validated by accurately simulating the response to a small earthquake. Non-linear dynamic analysis was performed with MSC/NASTRAN to investigate the error of modelling cables with beam elements in SASSI.

It was found that the response of the soil–structure system to the 1995 Hyogoken–Nanbu Earthquake had been strongly influenced by pore-water pressure buildup in the saturated surface soil layers. Non-linear effective stress analysis combining the Ramberg–Osgood stress–strain relation with a pore pressure model was performed to simulate the behaviour of the free-field soil. Excellent agreement was achieved.

Equivalent soil parameters were evaluated on the basis of the liquefaction analysis and were used to perform soil–structure interaction analysis with SASSI. A reasonably good agreement was achieved. Even though the equivalent linear soil parameters are not capable of producing a perfect simulation of the complicated non-linear behaviour, the results offer a reasonable accuracy for practical purposes.

REFERENCES

1. *Soils and Foundations* (Special Issue on the Geotechnical Aspects of the January 1995 Hyogoken–Nanbu Earthquake), Japanese Geotechnical Society, 1996.
2. H. T. Tang, J. Stepp, Y. Cheng, Y. Yeh, K. Nishi, T. Iwatate, T. Kokusho, H. Morishita, Y. Shirasaka, F. Gantenbein, J. Touret, P. Sollogoub, H. Graves and J. Costello, 'The Hualien Large-Scale Seismic Test for soil–structure interaction research', *Trans. 11th Int. Conf. on Structural Mechanics in Reactor Technology*, Vol. K, Tokyo, Japan, 1991, pp. 69–74.
3. T. Ganev, F. Yamazaki and T. Katayama, 'Observation and numerical analysis of soil–structure interaction of a reinforced concrete tower', *Earthquake Eng. Struct. Dyn.* **24**, 491–503 (1995).
4. T. Ganev, F. Yamazaki, T. Katayama and T. Ueshima, 'Soil–structure interaction analysis of the Hualien containment model', *Soil Dyn. Earthquake Eng.* **16**, 459–470 (1997).
5. J. Lysmer, F. Ostadan, M. Tabatabaie, S. Vahdani and F. Tajirian, *SASSI, A System for Analysis of Soil–Structure Interaction, User's Manual*, The University of California at Berkeley, CA, 1988.
6. Y. Yamada, N. Shiraishi, K. Toki, M. Matsumoto, K. Matsuhashi, M. Kitazawa and H. Ishizaki, Earthquake-resistant and wind-resistant design of the Higashi–Kobe Bridge, in M. Ito *et al.* (eds), *CABLE-STAYED BRIDGES, Recent Developments and their Future*, Elsevier, Amsterdam, 1991, pp. 397–416.
7. *Specifications for Highway Bridges*, Japan Road Association, 1990.
8. J. P. Wolf, *Dynamic Soil–Structure Interaction*, Prentice-Hall, Englewood Cliffs, 1985.
9. *MSC/NASTRAN for Windows*: *Installation and application manual*. The MacNeal-Schwendler Corporation, Los Angeles, USA, 1995.

10. T. Harada, K. Kubo and T. Katayama, 'Dynamic soil–structure interaction analysis by Continuum Formulation Method', *Report of the Institute of Industrial Science*, vol. 29, University of Tokyo, Japan, 1981.

11. K. Ishihara and I. Towhata, 'One-dimensional soil response analysis during earthquakes based on effective stress method', *J. Faculty Eng. Univ. Tokyo* (*B*) **35**(4), 655–700 (1980).

12. T. Katayama, F. Yamazaki, S. Nagata, L. Lu and T. Turker, 'A strong motion database for the Chiba seismometer array and its engineering analysis', *Earthquake Eng. Struct. Dyn.* **19**, 1089–1106 (1990).

13. I. Towhata and K. Ishihara, 'Shear work and pore water pressure in undrained shear', *Soils Found. JSSMFE* **25**(3), 73–84 (1985).

14. F. Yamazaki, I. Towhata and K. Ishihara, 'Numerical model for liquefaction problem under multi-directional shearing on a horizontal plane', *Proc. 5th Int. Conf. on Numerical Methods in Geomechanics*, Nagoya, Japan, 1985, pp. 399–406.